

" Structural, Magnetic and Dielectric Properties of Two Novel Mixed-Valence Iron(II)-Iron(III) Metal Formate Frameworks "

by M. Maczka *et al*

Table S1. Experimental details for $[C_2H_5NH_3][Fe^{II}Fe^{III}(HCOO)_6]$, **2**, and $[(C_2H_5)_2NH_2][Fe^{II}Fe^{III}(HCOO)_6]$, **3**.

	3	2
<i>Crystal data</i>		
Chemical formula	$C_{10}H_{18}Fe_2NO_{12}$	$C_8H_{14}Fe_2NO_{12}$
M_r	455.95	427.90
Crystal system, space group	Trigonal, $P-31c$	Trigonal, $P-31c$
Temperature (K)	260	298
a, c (Å)	8.4483 (2), 13.7058 (4)	8.2294(2), 14.1221(5)
V (Å ³)	847.18 (5)	828.26 (5)
Z	2	2
Radiation type	Mo $K\alpha$	Mo $K\alpha$
μ (mm ⁻¹)	1.77	1.81
Crystal size (mm)	$0.10 \times 0.05 \times 0.04$	$0.10 \times 0.08 \times 0.07$

Data collection

T_{min}, T_{max}	0.925, 1.000	0.874, 1.000
No. of measured, independent and observed	10788, $[I > 542,$	8996, 527,

$2\sigma(I)$] reflections	482	459
R_{int}	0.033	0.032
$(\sin \theta / \lambda)_{\text{max}} (\text{\AA}^{-1})$	0.610	0.610

Refinement

$R[F^2 > 2\sigma(F^2)]$, 0.029, 0.079, 1.08	0.038, 0.113, 1.09	
$wR(F^2), S$		
No. of reflections	542	
No. of parameters	43	
No. of restraints	4	
H-atom treatment	H-atom parameters constrained	H-atom parameters constrained
$\Delta\rho_{\text{max}}, \Delta\rho_{\text{min}} (\text{e \AA}^{-3})$	0.55, -0.35	1.00, -0.54

Table S2. IR frequencies (in cm^{-1}) of **2** and **3** together with the suggested assignments.^a

3		2		Assignment
298 K	4 K	298 K	4 K	
3354sh	3352sh			v(NH ₃) and v(NH ₂)
3305w	3302m	3276sh	3277sh	v(NH ₃) and v(NH ₂)
3213sh	3207sh	3201w	3216m, 2196sh	v(NH ₃) and v(NH ₂)
3175m	3171m	3133vw	3127w	v(NH ₃) and v(NH ₂)
3106m	3071m, 3037m	3080w	3077m	v(NH ₃) and v(NH ₂)
3012w	3007m	3019vw	3016w	v(CH ₃) and v(CH ₂)
3001w	2999m	3000vw	2996w	v(CH ₃) and v(CH ₂)
2983w	2979w	2987vw	2982w	v(CH ₃) and v(CH ₂)
2971w	2972w	2969vw	2977w	v(CH ₃) and v(CH ₂)
2957w	2959w			v(CH ₃) and v(CH ₂)
2942w	2938m	2946w		v(CH ₃) and v(CH ₂)
			2929m	v(NH ₃)
2910vw	2919sh, 2904w			v(CH ₃) and v(CH ₂)
2898vw	2898w			v(CH ₃) and v(CH ₂)
2875m	2882m	2881w	2884m, 2877sh	$\nu_1(\text{HCOO}^-)$
2864sh	2868m, 2857m			$\nu_1(\text{HCOO}^-)$
2826w	2830w, 2818sh			overtone
	2813w			
		1626sh	1628sh	$\delta_{\text{as}}(\text{NH}_3)$
1586s	1587s, 1570sh	1585s	1589s, 1574s	$\nu_4(\text{HCOO}^-)$
	1560sh			
		1485w	1487w	$\delta_s(\text{NH}_3)$
1473vw	1476w, 1464vw	1463w	1458w	$\delta(\text{CH}_3)$ and $\delta(\text{CH}_2)$

		1459vw		
1453w	1450m	1451w	1447w	$\delta(\text{CH}_3)$ and $\delta(\text{CH}_2)$
1447w	1441m	1447w	1444m	$\delta(\text{CH}_3)$ and $\delta(\text{CH}_2)$
	1425w			$\omega(\text{NH}_2)$
	1408vw			$\tau(\text{NH}_2)$ and $\delta_s(\text{CH}_3)$
1394m	1395m	1386s	1395s, 1388s	$\nu_5(\text{HCOO}^-)$
1383m	1387m			$\nu_5(\text{HCOO}^-)$
1378m	1382m, 1380m			$\nu_5(\text{HCOO}^-)$
	1374m			$\nu_5(\text{HCOO}^-)$
	1366vw		1367sh	$\nu_2(\text{HCOO}^-)$
1346s	1349s, 1343m	1347s	1348s	$\nu_2(\text{HCOO}^-)$
	1334s			
		1328sh	1333sh	$\nu_2(\text{HCOO}^-)$
1261sh	1269w	1222w	1227w	$\rho(\text{CH}_3)$ and $\rho(\text{CH}_2)$
1195w	1202w	1194w	1196w	$\rho(\text{CH}_3)$
1158vw	1167vw, 1160vw			overtones
	1155vw			
1072w	1073w			$\rho(\text{CH}_3)$
1058w	1061sh, 1057w			$\nu_6(\text{HCOO}^-)$
1055w	1057m, 1048sh	1051w	1057w	$\nu_6(\text{HCOO}^-)$
			1044w	$\nu_{\text{as}}(\text{C-C})$ and $\nu_{\text{as}}(\text{C-N})$
1032w	1032vw			$\rho(\text{CH}_3)$
1024w	1025w			$\rho(\text{CH}_3)$
		992w	998w	$\rho(\text{NH}_3)$
		964w	960w	$\rho(\text{NH}_3)$
907vw	922w			$\nu_{\text{as}}(\text{C-C})$ and $\nu_{\text{as}}(\text{C-N})$

896w	906w			$\nu_{as}(C-C)$ and $\nu_{as}(C-N)$
		870vw	870vw	$\nu_s(C-C)$ and $\nu_s(C-N)$
	866w			$\rho(NH_2)$
	845vw			$\nu_s(C-C)$ and $\nu_s(C-N)$
810m	817m, 808sh	815m	820m	$\nu_3(HCOO^-)$
790w	788m	785m	781m	$\nu_3(HCOO^-)$
782w	782m			$\nu_3(HCOO^-)$
761w	762w			overtone
665vw	663vw, 639w			overtone

^aKey: s, strong; m, medium; w, weak; vw, very weak; sh, shoulder

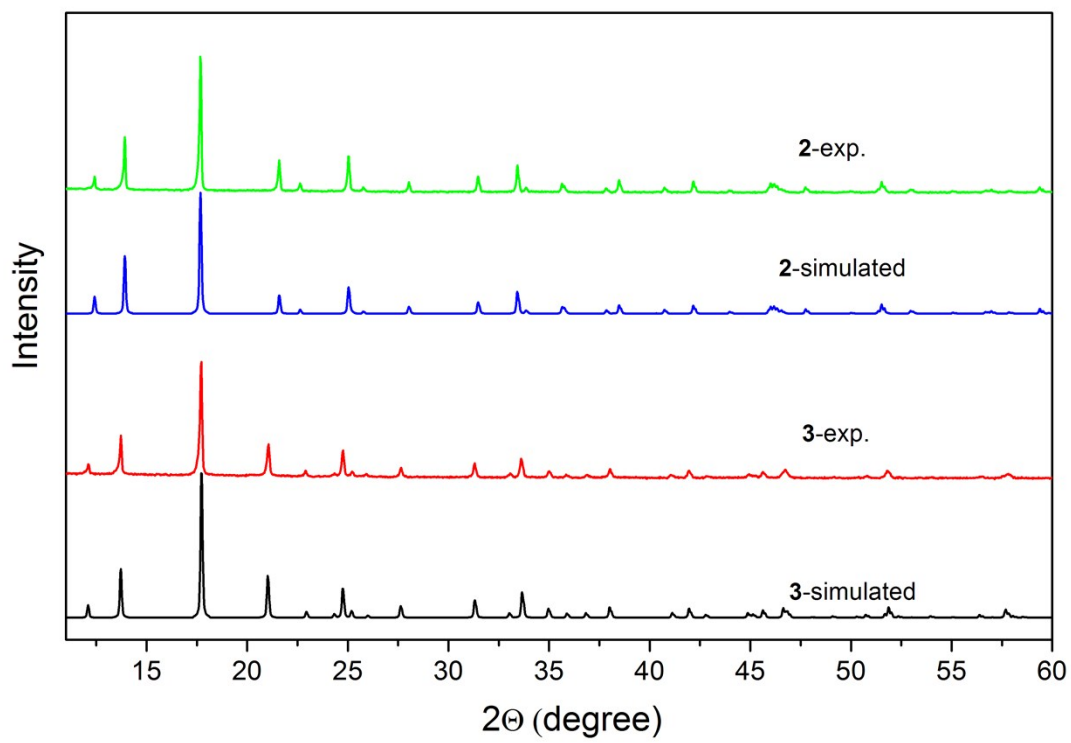


Figure S1. Powder XRD patterns for the as-prepared bulk samples of **2** and **3** with the calculated ones based on the single crystal structures at room temperatures.

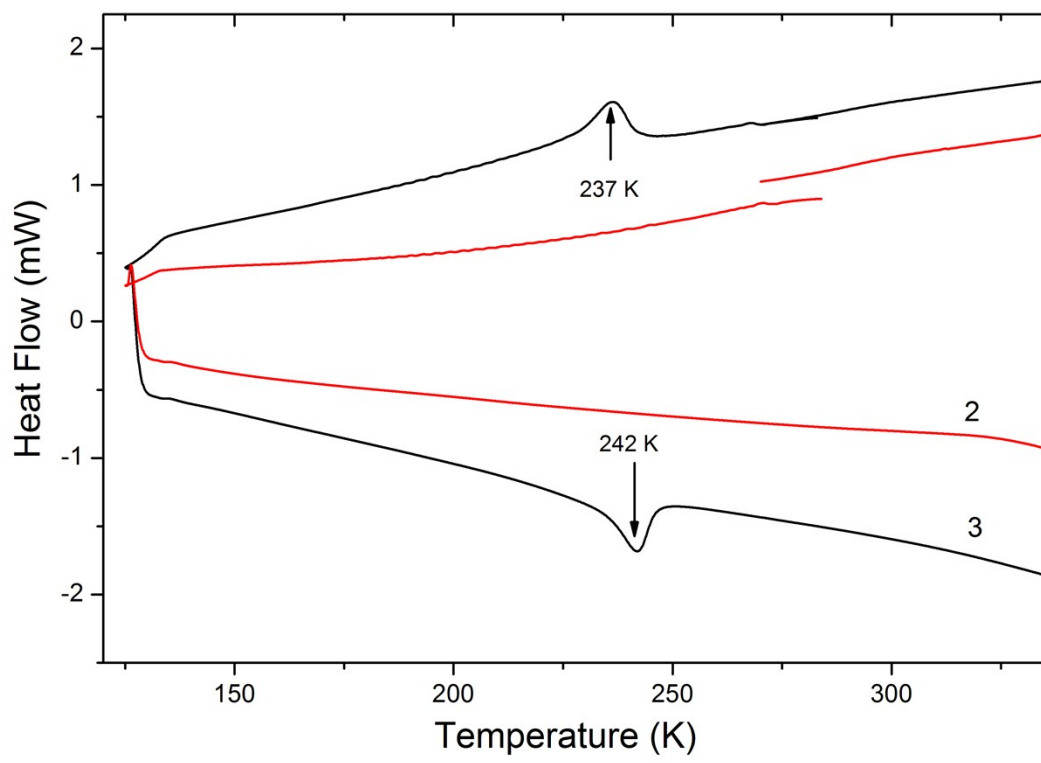


Figure S2. DSC traces for **2** and **3** in heating and cooling modes.

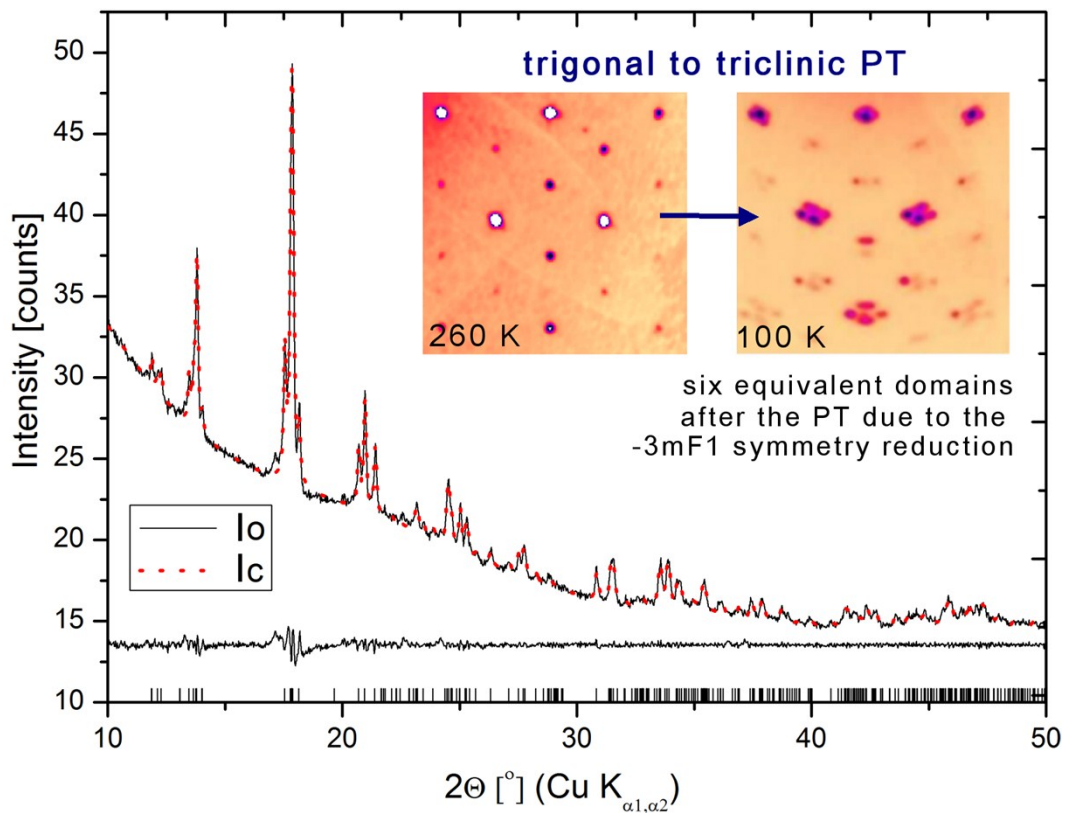


Figure S3. The results of the Le Bail fit of the XRD pattern in phase II of **3** using a triclinic unit cell with parameters $a=8.307(1)\text{\AA}$, $b=8.585(1)\text{\AA}$, $c=13.540(1)\text{\AA}$, $\alpha=89.5(1)$, $\beta=89.3(1)$, $\gamma=119.7(1)$, $T=205$ K. The residuals between the fits and the positions of the Bragg peaks are given in the bottom. In the inset the reciprocal space reconstruction of $hk0$ layer in phase I and II are presented. The phase transition (PT) to the triclinic phase induces lattice twinning to six equivalent domains. I_o, I_c : observed and calculated intensity.

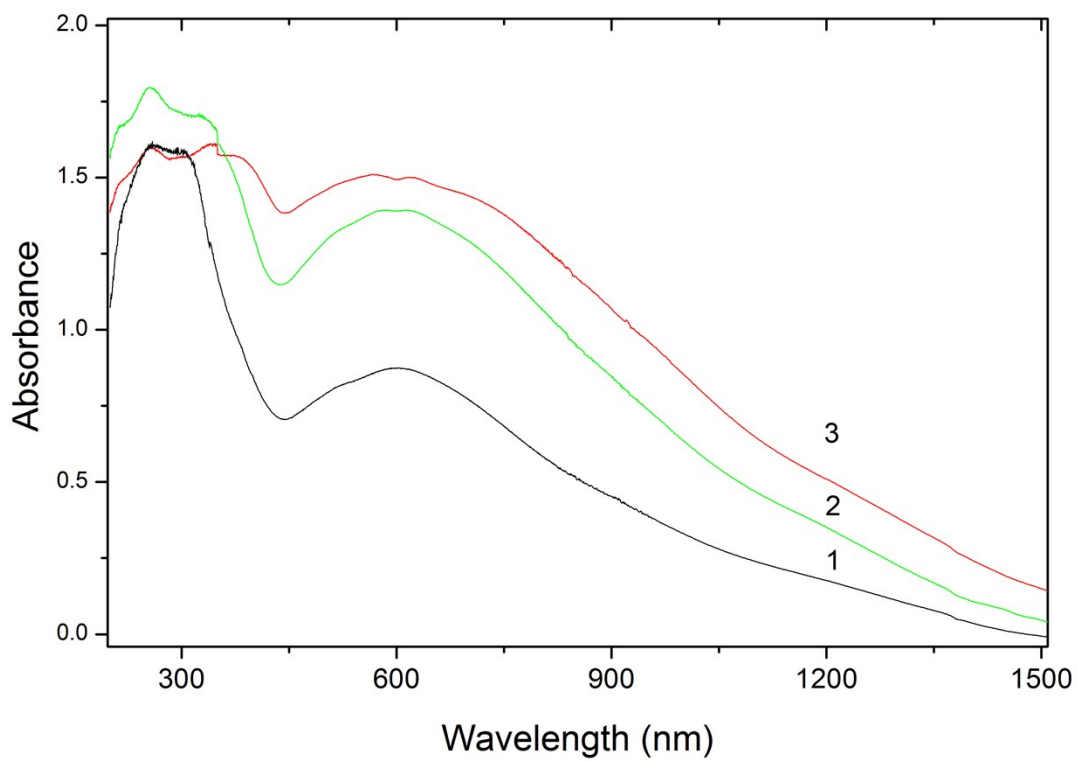


Figure S4. Diffuse reflectance spectra of **2** and **3**. For the comparison sake, spectrum of **1** is also shown.

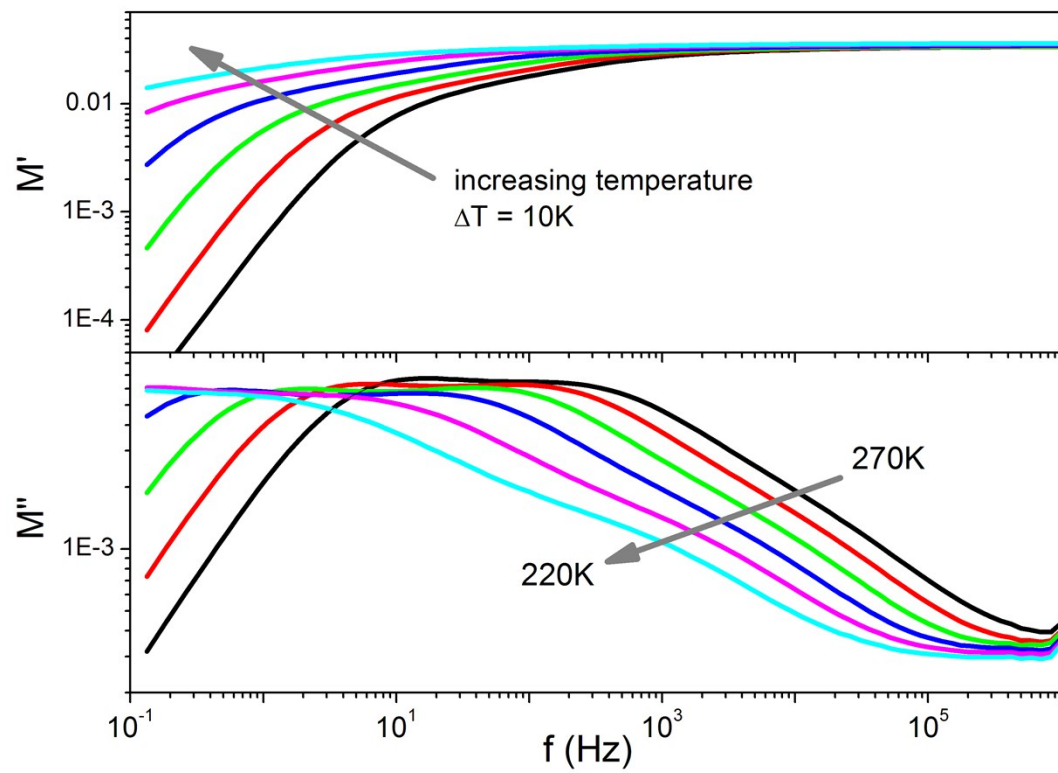


Figure S5. The frequency dependence of the real M' and imaginary M'' parts of the electric modulus for 3.

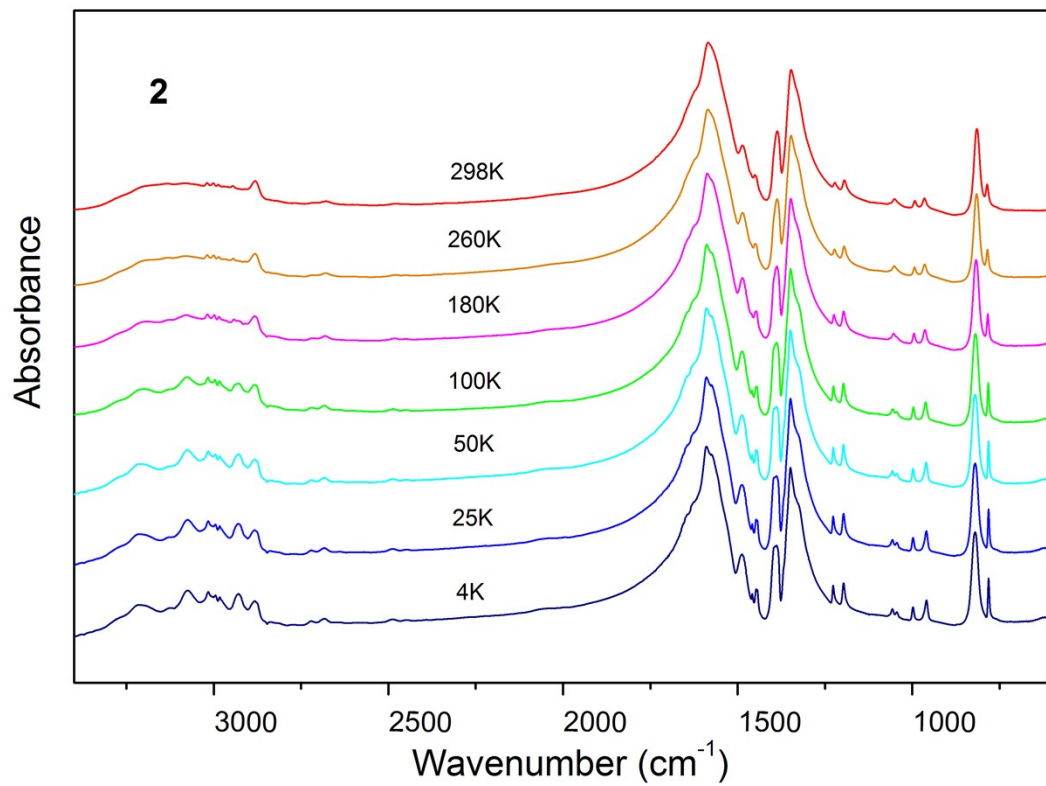


Figure S6. IR spectra of **2** recorded at various temperatures.

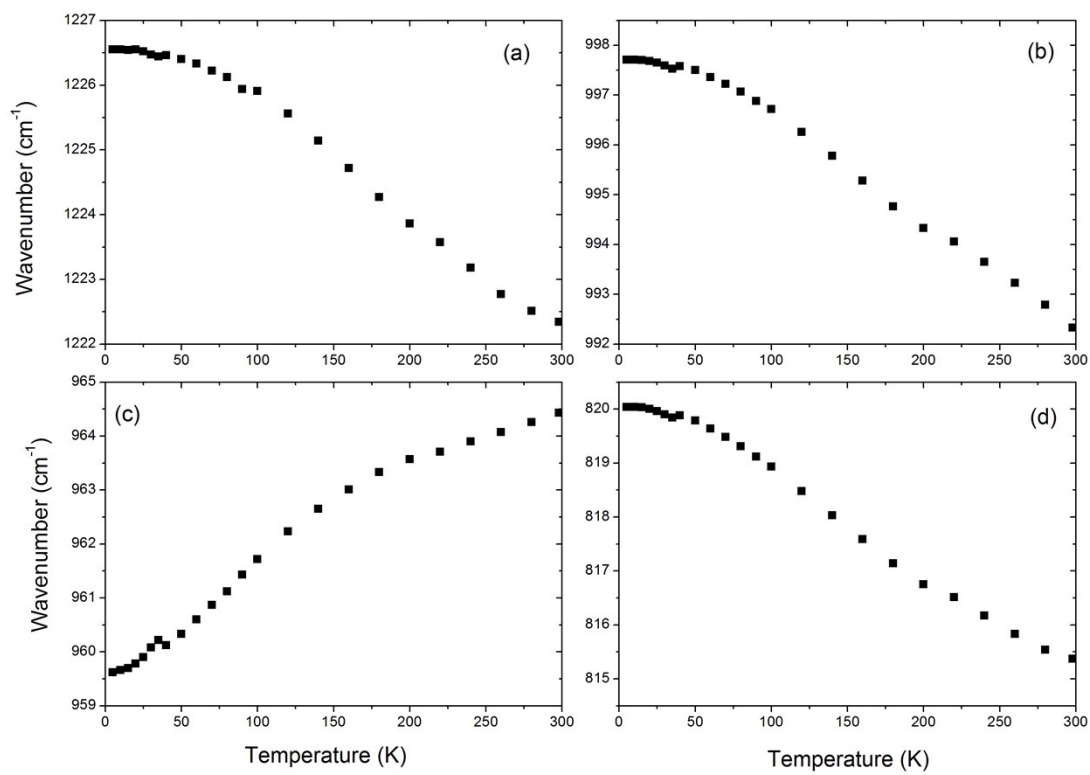


Figure S7. Temperature evolution of a few selected IR wavenumbers of **2** corresponding to (a) $\rho(\text{CH}_3)$ and $\rho(\text{CH}_2)$; (b) $\rho(\text{NH}_3)$; (c) $\rho(\text{NH}_3)$ and (d) $\nu_3(\text{HCOO}^-)$ modes.

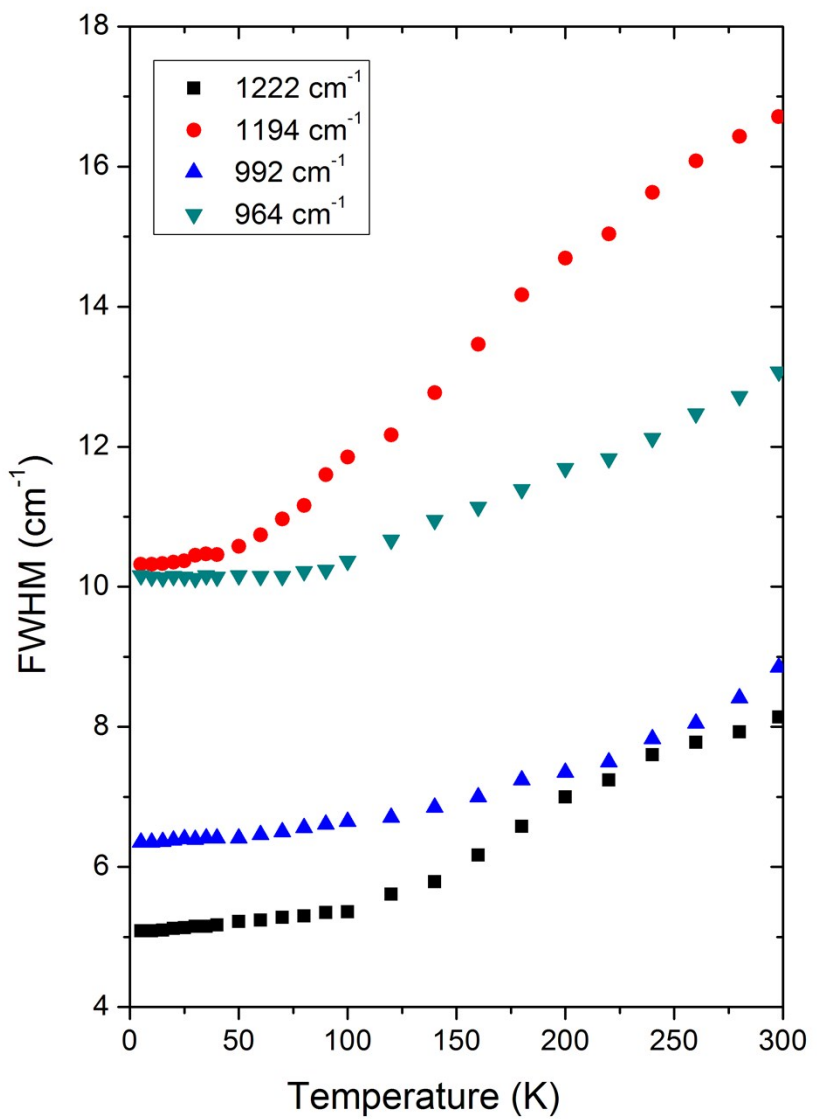


Figure S8. FWHM as a feunction of temperature for a few selected IR modes of **2**.

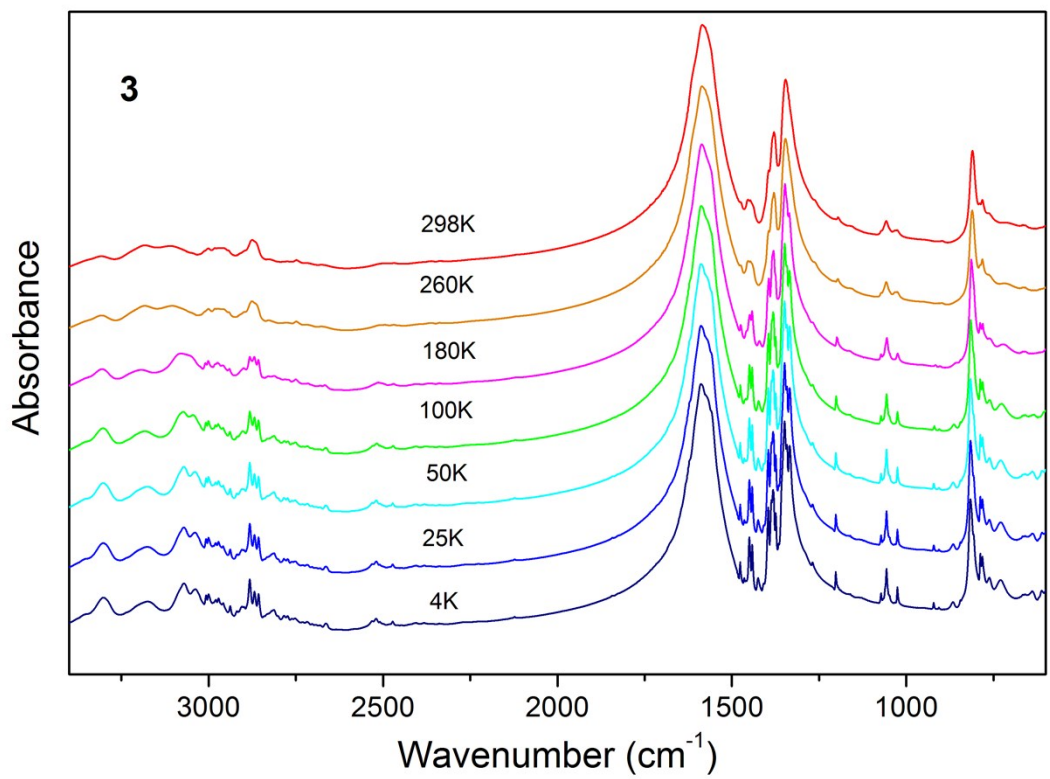


Figure S9. IR spectra of **3** recorded at various temperatures.

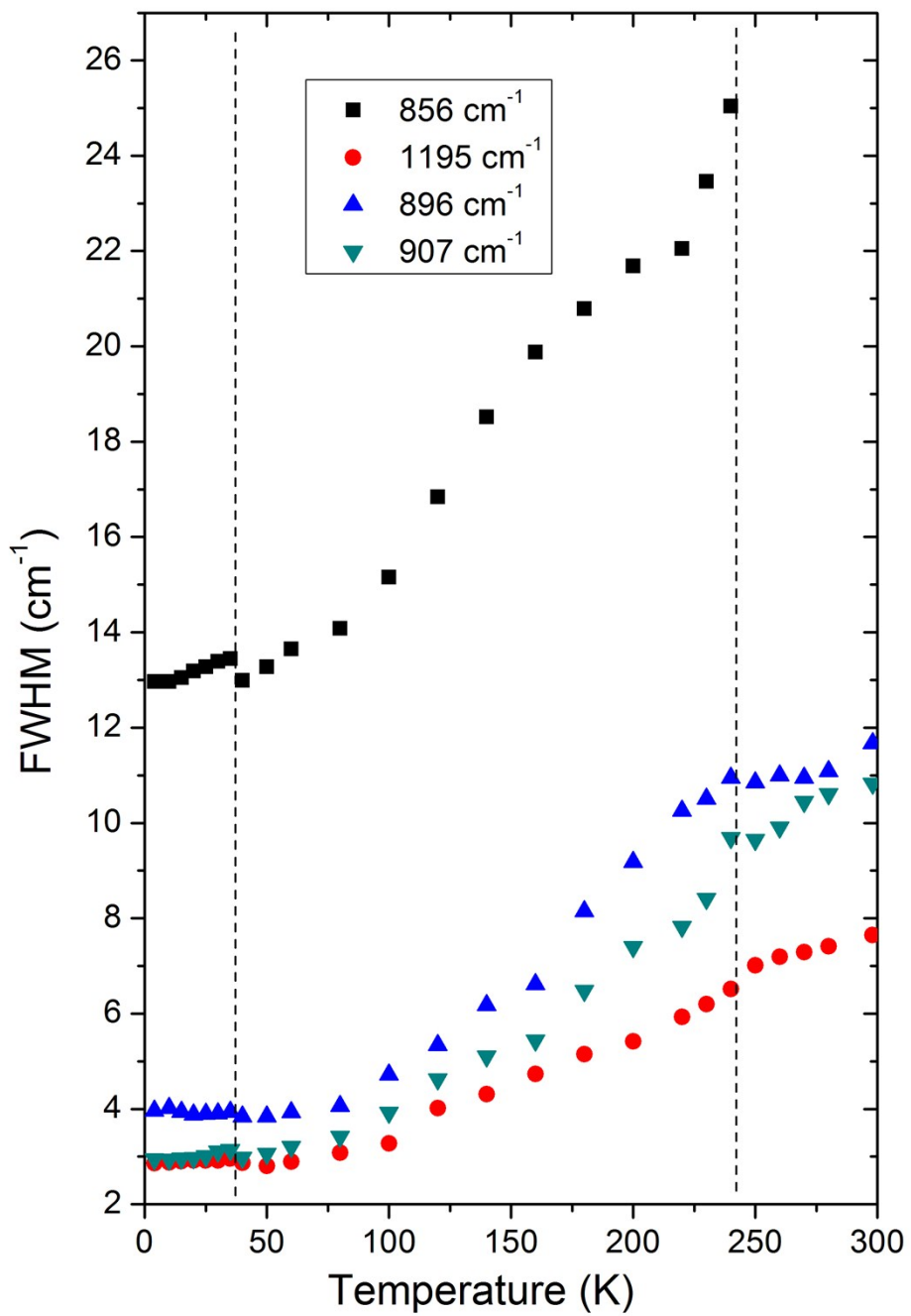


Figure S10. FWHM as a function of temperature for a few selected IR modes of **3**. Vertical lines indicate temperatures of the structural and magnetic phase transitions.